V International Conference on Particle-based Methods – Fundamentals and Applications
PARTICLES 2017
P. Wriggers, M. Bischoff, E. Oñate, D.R.J. Owen, & T. Zohdi (Eds)

HYDRODYNAMIC LOADS SIMULATION FOR 3D BLUFF BODIES BY USING THE VORTEX LOOPS BASED MODIFICATION OF THE VORTEX PARTICLE METHOD

GEORGY A. SHCHEGLOV AND SERGEY A. DERGACHEV

Bauman Moscow State Technical University (BMSTU)
2-nd Baumanskaya st., 5, 105173 Moscow, Russia
E-mail: shcheglov_ga@bmstu.ru

Key words: 3D incompressible flow, vortex method, closed vortex loop, bluff body, pressure distribution.

Summary. *The modification of vortex method is developed which is based on closed vortex loops usage for calculation of unsteady aerodynamic loads acting on bluff bodies. It is shown that such approach has number of advantages for vortex wakes evolution simulation after bluff bodies. Each vortex loop can be considered as the separate vortex "superelement", which doesn't generate any additional vorticity. The loops generation algorithm permits to simulate the separation zone due to the self-organization of the loops. The obtained results are in satisfactory agreement with known experimental data.*

1 INTRODUCTION

For calculation of unsteady aerodynamic loads acting on aircraft moving at low subsonic speed vortex methods are highly efficient, as they require significantly less computational resources in comparison with grid-based methods. There are number of models of vortex elements known for flow simulation around spatial bodies: closed vortex framework, vortex filament, vorton, vortex dipole, vortex fragmenton, etc. Each of them has some advantages and restrictions.

In 'classical' vortex element methods, for example, in the discrete vortex method [1], vorticity is concentrated in vortex framework segments and it is absent outside the filaments segments in the flow. However, this method requires number of empirical models to determine the location of the vortex sheet separation lines. In case of vortex methods with separated vortex particles flow separation regions are being formed 'naturally' due to vorticity flux approach – vortex elements generation on the whole streamlined surface and further self-organization of the vortons in the flow [2, 3]. The main part of the vorticity is concentrated close to vortex elements (vortons) at points or at line segments. However, in the flow domain, according to the Helmholtz theorems, there will be distributed non-zero 'additional' vorticity. Its intensity vanishes on infinity [4]. This additional vorticity may cause significant errors when computing aerodynamic loads acting the body. Recently, there have been proposed an approach according to which the vorticity flux is being simulated by vortex filament loops generation on the body surface for 3D smoke dynamics simulation [5].

The aim of this paper is validation of vortex element method modification based on closed vortex loops usage for calculation of unsteady aerodynamic loads acting on bluff bodies.

2 PROBLEM STATEMENT AND NUMERICAL METHOD DESCRIPTION

The incompressible 3D flow around fixed rigid body is considered. The flow of the media, which has small viscosity and constant density ρ_∞ is described by the continuity equation and momentum equation with no-slip boundary condition on the body surface and perturbation decay boundary condition on infinity. Initial conditions correspond to the circulation-free flow. It is necessary to find the unknown pressure distribution on the body surface.

The assumption about incompressibility of the flow allows to find the velocity field $\vec{V}(\vec{r},t)$ by using the Biot – Savart law from vorticity distribution $\vec{\Omega} = \nabla \times \vec{V}$ with automatic satisfaction of boundary conditions on infinity. The pressure field also can be found from vorticity distribution by using analog of the Cauchy – Lagrange integral [6]. The assumption about viscosity smallness allows to take its influence into account only for simulation of two processes: the vorticity flux near body surface and vortex filaments reconnection in the flow.

For the lagrangian description of vorticity evolution the momentum equation has the following form:

$$\frac{D\vec{r}}{Dt} = \vec{V}, \qquad \frac{D\vec{\Omega}}{Dt} = (\vec{\Omega}\cdot\nabla)\vec{V}\ , \tag{1}$$

where $\vec{r}$ is vorticity markers positions. No-slip boundary condition is satisfied by implementing of vorticity flux approach [7, 8]. Boundary vortex sheet intensity can be found from no-through condition on body surface $\vec{r}_K$ with unit normal vector $\vec{n}_K$

$$\vec{V}_K \cdot \vec{n}_K = 0\,. \tag{2}$$

Then vortex sheet is being transformed into vorticity $\vec{\Omega}_K$, which is added to the vortex wake in the flow.

The developed vortex element method modification is based on the closed vortex loops usage for numeric solution of system (1) with condition (2) on time interval $0 \le t \le T$. Vortex wake consists of the K closed vortex filaments – vortex loops of the same circulation Γ. Loop with number $k \in [1,K]$ is simulated by the polygonal vortex line with number of vertices N_k. Vertices of a polyline with number $i \in [1,N_k]$ are considered as the Lagrangian markers $\vec{r}_{ki}$. The markers motion is described by ODE:

$$\frac{d\vec{r}_{ki}}{dt} = \vec{V}_{ki}, \quad \vec{r}_{ki}(0) = \vec{r}^{\,o}_{ki}, \quad i = 1,...,N_k, \quad k = 1,...,K\,. \tag{3}$$

We assume the loop legs between two vertices to be rectilinear segments $\Delta\vec{r}_{ki} = \vec{r}_{ki+1} - \vec{r}_{ki}$ and they induce the velocity $\vec{v}_{ki}(\vec{r})$ in the flow as vortex fragmentons, regularized by introducing of small smoothing radius ε [5].

For boundary condition (2) satisfaction linear system

$$[\sigma]\{\gamma\} = \{V_n\}, \tag{4}$$

should be solved for unknown circulations γ_j ($j \in [1,N_p]$) of vortex fragmenton frameworks,

placed on N_p body surface panels. For solving of (4) the regularization variable and additional condition is used: algebraic sum of vortex frameworks circulations should be equal to zero.

Finally, the velocity of the *i*-th marker of the *k*-th loop has the form

$$\vec{V}_{k\,i} = \vec{V}_\infty + \Gamma \sum_{l=1}^{K} \sum_{m=1}^{N_k} \vec{v}_{lm}\left(\vec{r}_{k\,i}\right) + \sum_{j=1}^{N_p} \gamma_j \sum_{s=1}^{N_j} \vec{v}_{sj}\left(\vec{r}_{k\,i}\right), \tag{5}$$

where $\vec{V}_\infty$ - constant incident flow velocity; N_j - number of vortex fragmentons in *j*-th vortex framework.

Numerical integration of system (3) is carried out by using numerical method of the first order of accuracy (explicit Euler method) with constant step Δt. Initial conditions for markers positions in (3) are parameters of the loops at the time of their generation on surface of the streamlined body. At every time step several procedures for smoothing of loops geometry, loop segments length alignment and loops reconnection are used [9]. Vortex loops generation algorithm is described below.

Pressure field at every time step is being calculated from the positions of loops by using the analog of the Cauchy – Lagrange integral. Aerodynamic loads are determined by integration of the pressure distribution over the surface of the body. In this research stationary loads are computed by averaging over the period of simulation. To implement the numerical method, the C++ program was developed, which uses MPI technology for parallel computations.

3 VORTEX LOOPS GENERATION ALGORITHM

Vortex loops generation algorithm consists of three main operations:

1. *Vortex sheet generation.* By solving of (4) circulations of vortex frameworks on the body panels can be found.

2. *Vortex loops construction.* Firstly, maximal and minimal intensities $M = \max(\gamma_j)$ and $m = \min(\gamma_j)$ should be found. Then each *j*-th panel should be split into N_j triangles (Fig.1). The potential scalar function is being introduced on the body surface, and its values at the control points of the panels are equal to the circulations of the corresponding vortex frameworks: $G_j = \gamma_j$. Its values at the corners of the framework are defined by circulations averaging for the frameworks which are adjacent to this point. For example, for the quadrangular panel shown in fig. 1:

$$\Phi_2 = (\gamma_1 + \gamma_2 + \gamma_3 + \gamma_4)/4 \tag{6}$$

The potential distribution over the triangle with known values at vertices is determined by linear interpolation. Potential level lines determine the initial shape of the vortex loops. For each value of the potential there can one or more closed level lines, each of them corresponds to one vortex loop. The number of level lines is determined as the integer part of expression

$$N_q = [(M - m)/\Gamma] - 1 \tag{7}$$

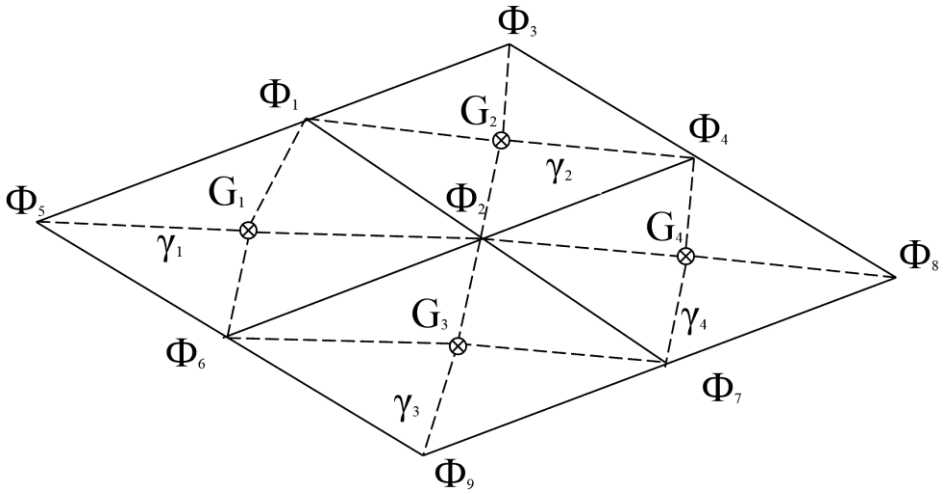

Figure 1: Example of splitting of a vortex framework into triangles

3. *Vortex loops dropping.* The constructed vortex loops should be shifted from the surface in the direction of a normal on small constant distance Δ. These new loops are being added to vortex wake loops database. On the current step, after generation of a loop, its contribution to the velocity field (5) is not considered, and for velocity field influence of the corresponding framework on body surface is taken into account.

When vortex elements move in the flow, marker positions of some of them can appear inside the body due to numerical errors. In such cases, the loop's leg, which intersects the body surface, is replaced with the other loop legs, which lay on the body surface and provide the shortest way by means of Dijkstra's algorithm [10].

4 MODEL PROBLEMS DESCRIPTION

For validation of the developed algorithm, several model problems are considered. The first problem is flow simulation around a sphere of unit radius. On the surface of the corresponding geometric model a mesh consists of $N_p = 1917$ triangular frameworks ($N_j = 3$) was built. The smoothing radius of the vortex element was chosen equal to $\varepsilon = 0.004$, time integration step $\Delta t = 0.01$, the length of the segment with which the loop was constructed $\alpha = 0.01$; the constant circulation of the vortex loop $\Gamma = 0.03$. The parameters of the algorithm [9] for simulation of the evolution of vortex loops are the following: nominal length of loop segment $h = 0.01$, loop smoothing angle threshold $\varphi = 160°$, loops reconnection distance $\mu = 0.015$, length decreasing coefficient $\lambda = 1.3$, number of segments in reconnection zone $\Omega = 7$. The number of loops in the wake at the end of simulation was equal to $K = 104$. The total number of segments in the wake was around 77 700. The shape of a vortex loops in the wake at the end of the simulation is shown in Fig.2.

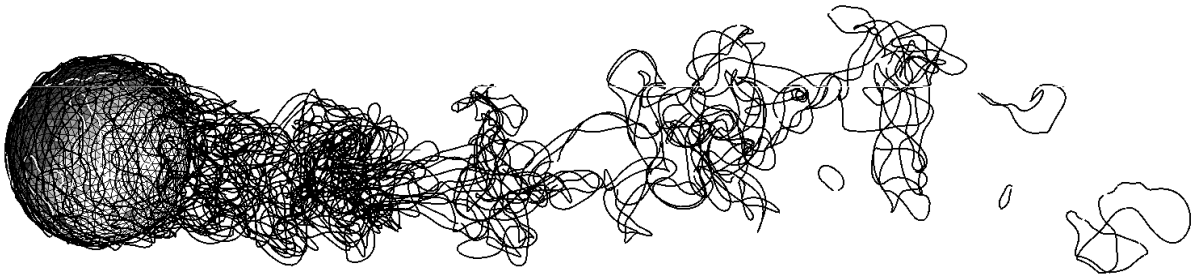

Figure 2: Vortex wake consists of closed vortex loops past the sphere

On Fig.3 the comparison of calculated results with the experiment [11] is shown: solid line – the dependence of the pressure coefficient C_p on the angular coordinate ϕ (in radians). Zero value of the x-axis of this diagram corresponds to the flow stagnation point. Dotted line denotes the experimental results for the Reynolds number $\mathrm{Re} = 10^6$ and dashed line denotes the experimental results for $\mathrm{Re} = 10^4$. The calculation time of 500 steps on 6 computers with Quad core Intel I7 3.0 GHz was about 4 hours, which yields a speedup of 3.5 times compared to the program used in [5].

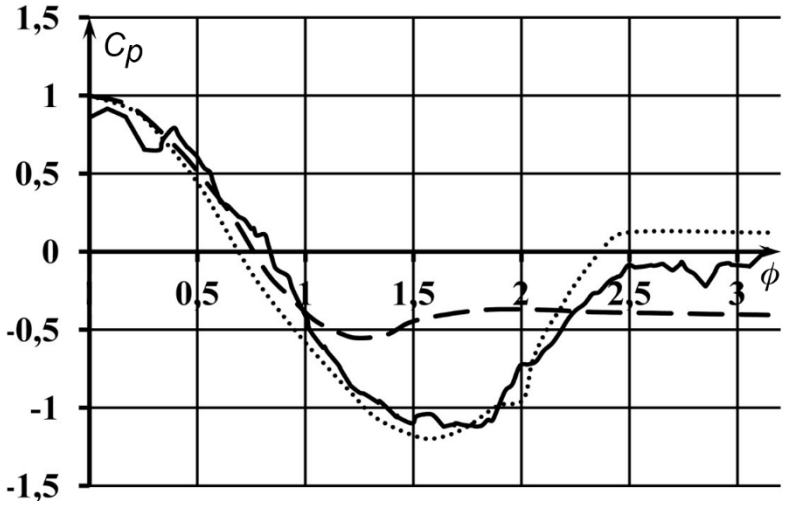

Figure 3: Dependence of the pressure coefficient for the sphere in comparison with experiment [11]

The second model problem is flow simulation around a circular cylinder with dimensions $D = 0.2$, $L = 2.55$. On the surface of the corresponding geometric model a mesh consists of $N_p = 4570$ triangular frameworks ($N_j = 3$) was built. The model parameters are the following: $\varepsilon = 0.001$, $\Delta t = 0.0044$, $\alpha = 0.01$; $\Gamma = 0.005$, $h = 0.01$, $\varphi = 160°$, $\mu = 0.015$, $\lambda = 1.4$, $\Omega = 7$. The number of loops in the wake at the end of simulation was equal to $K = 35$. The total number of segments in the wake was around 70 000. The shape of a vortex loops in the wake at the end of the simulation is shown in Fig.4.

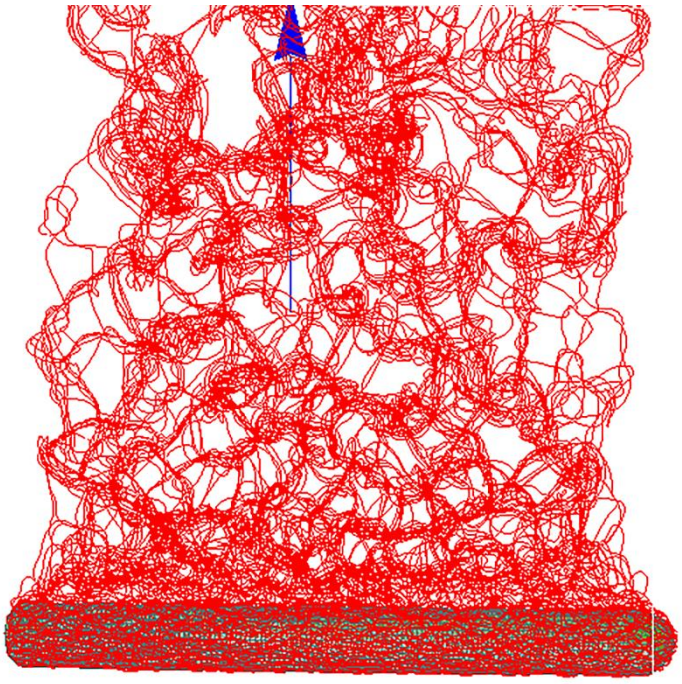

Figure 4: Vortex wake consists of closed vortex loops past the cylinder

On Fig.5 the comparison of calculated results with the experiment [12] is shown: solid green line is the dependence of the pressure coefficient C_p on the angular coordinate ϕ (in radians). Zero value of the x-axis of this diagram corresponds to the flow stagnation point. Blue line denotes the experimental results for the Reynolds number $\mathrm{Re} = 10^4$, violet line denotes the experimental results for $\mathrm{Re} = 10^5$ and red line denotes the experimental results for $\mathrm{Re} = 10^6$.

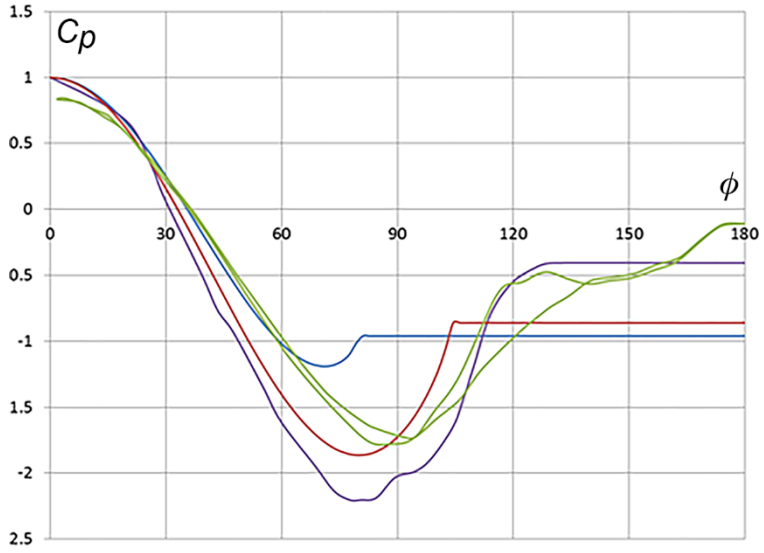

Figure 5: Dependence of the pressure coefficient for the sphere in comparison with experiment [12]

5 CONCLUSIONS

The validation of the developed modification of vortex element method with closed vortex loops showed that it has number of advantages for simulation of the evolution of vortex wakes behind bluff bodies:

- Each vortex loop can be considered as the separate vortex "superelement", which does not generate any additional vorticity.
- The loops generation algorithm allows to simulate the separation zone due to the self-organization of loops.

The obtained results are in satisfactory agreement with known experimental data. Further research will be devoted to the analysis of the influence of model parameters on the accuracy of the results and improvement of software code.

REFERENCES

[1] Belotserkovsky, S.M. et al. *3D detached flows around bodies of arbitrary shape*. Moscow, TSAGI, (2000). (In Russian: *Trekhmernoe otrihvnoe obtekanie tel proizvoljnoyj formi*).

[2] Kamemoto, K. On Contribution of Advanced Vortex Element Methods Toward Virtual Reality of Unsteady Vortical Flows in the New Generation of CFD. *J. of the Brazilian Society of Mechanical Sciences and Engineering.* (2004) V. 26, No 4.: 368-378.

[3] Alkemade, A.J.Q. *On Vortex Atoms and Vortons*: PhD Thesis. Delft, (The Netherlands), (1994).

[4] Marchevsky, I.K. and Shcheglov, G.A. 3D vortex structures dynamics simulation using vortex fragmentons. *ECCOMAS 2012, e-Book Full Papers, Vienna*, (2012): 5716–5735.

[5] Weißmann, S. and Pinkall, U. Filament-based smoke with vortex shedding and variational reconnection. *ACM Trans. Graph*. (2010) Vol. 29, No 4, article 115. 12 p.

[6] Dynnikova, G.Ya. An analog of the Bernoulli and Cauchy-Lagrange integrals for a time-dependent vortex flow of an ideal incompressible fluid. *Fluid Dynamics.* (2000) Vol. 35, No 1: 24-32.

[7] Lighthill, M.J. Introduction. *Boundary Layer Theory Laminar Boundary Layers Ed. by J. Rosenhead*. New-York: Oxford University Press, (1963): 54-61.

[8] Kempka, S.N., Strickland, J.H., Glass, M.W. and Peery, J.S. *Accuracy Considerations for Implementing Velocity Boundary Conditions in Vorticity Formulations* Sandia Report. SAND96-0583 UC-700. (1996)

[9] Dergachev, S.A. and Shcheglov, G.A. Flow around 3D bodies simulation by using vortex element method with closed vortex loops. *Heralds of MGTU GA.* (2016) No 223 (1): 19-25. (in Russian)

[10] Dijkstra, E.W. A note on two problems in connexion with graphs. *Numerische Mathematik.* (1959) Vol.1: 269-271.

[11] Flachsbart, O. Der Widerstand von Kugeln in der Umgebung der kritischen Reynoldschen Zahl. *Ergebnisse der Aerodynamischen Versuchsanstalt zu Göttingen.* IV. Lieferung, (1932): 106-108.

[12] Parkinson, G.V. and Jandali, T. A wake source model for bluff body potential flow *J. of Fluid Mechanics* (1970), Vol. 40, No. 3: 577-594